

³¹Calculated from a diffusion activation energy of 2.5 eV given by L. L. Chang and G. L. Pearson, *J. Appl. Phys.* **35**, 374 (1964) and from an estimate for the rate of interstitial diffusion of $\sim 10^{-4}$ cm²/sec at $\sim 1200^\circ\text{K}$ given by L. L. Chang and G. L. Pearson, *J. Appl. Phys.* **35**, 1960 (1964). It can be noted that the 2.5 eV was obtained at high temperatures, with a lower activation en-

ergy at lower temperatures, but S. F. Nygren and G. L. Pearson [*J. Electrochem. Soc.* **116**, 648 (1969)] have since attributed the low-temperature results to diffusion along dislocations; such diffusion is obviously of no relevance to the present work.

³²D. Redfield, *Phys. Rev.* **130**, 914 (1963).

Identification of Γ Transitions in the E'_0 Region of Germanium by Piezoreflectance Measurements

D. D. Sell and E. O. Kane

Bell Laboratories, Murray Hill, New Jersey 07974

(Received 7 July 1971)

The reflectance of germanium and its logarithmic derivative $(dR/dE)/R$ in the 2.8- to 4.0-eV spectral region have been reexamined as a function of temperature (2 to 300 K) and uniaxial stress. Two relatively sharp structures at 3.00 and 3.19 eV are seen in the unstressed derivative data at 2 K. The observed splittings and polarizations of these two structures for large uniaxial stress along [001] or [111] directions agree well with the behavior calculated for $\Gamma_5^v \rightarrow \Gamma_7^c$ and $\Gamma_8^v \rightarrow \Gamma_8^c$ transitions, respectively. The data are incompatible with a Δ symmetry assignment for these two structures. A third broader structure is seen near 3.5 eV, the expected energy for a $\Gamma_7^v \rightarrow \Gamma_8^c$ transition; however, the temperature independence and strength of this structure indicate that it is not a Γ transition.

I. INTRODUCTION

Structures commonly denoted as E_0 , E_1 , E'_0 , and E_2 have been observed in a large number of semiconductors in groups IV, III-V, and II-VI.¹ Of these, the E_0 (at Γ) and E_1 (along Λ) have been studied extensively and are reasonably well understood. In comparison, the E'_0 and E_2 regions have received relatively little attention and the nature of these transitions has not been thoroughly established. In this paper we are concerned with the E'_0 region in germanium. E'_0 structure near 3.1 eV was seen in the early reflectance data of Philipp and Taft² and the transmission data of Cardona and Harbeke.³ In later work Potter⁴ (oblique-angle reflectance) and Ghosh⁵ (electroreflectance) reported additional structures in the 2.6–3.2-eV region. Zucca and Shen⁶ and Braunstein and Welkowski⁷ studied the reflectance in this region by the wavelength-modulation technique. In general, the observed structure is weak and relatively difficult to study. The data obtained by the different techniques, and the interpretations of these data, are not completely compatible. These results do not provide the evidence needed to identify the observed structure with particular electronic transitions. Band calculations associate the E'_0 structure with transitions at,⁸ or near,⁹ Γ ($\Gamma_5^v \rightarrow \Gamma_5^c$)¹⁰ or possibly with $\Delta_5 \rightarrow \Delta_1$ transitions along an extended region of the Δ -symmetry line.^{11,12}

Recently, Fischer and co-workers¹³ have pre-

sented direct evidence from transverse electroreflectance and photoemission experiments which identifies a portion of the E'_0 structure in germanium as $\Gamma_5^v \rightarrow \Gamma_5^c$ transitions. Their results prompted us to reexamine the reflectance in this region at low temperatures as a function of large uniaxial dc stress. The splittings and polarization behavior which we observe for [111] and [001] stress provide conclusive proof that their assignments are correct. At 2 K the 3.00- and 3.19-eV structures are $\Gamma_8^v \rightarrow \Gamma_7^c$ and $\Gamma_8^v \rightarrow \Gamma_8^c$ transitions, respectively. Our data are incompatible with a Δ -symmetry assignment for these transitions.

These results are important for two reasons: First, the transition energy provides an additional parameter for band calculations which determines the position of the second conduction band at the center of the zone. Second, in view of the similarity of semiconductor spectra, our results for germanium suggest that similar results may be observed in other materials.

II. SYMMETRY ANALYSIS OF Γ TRANSITIONS FOR [001] AND [111] STRESS

In this section we consider the polarization selection rules for optical transitions between Γ_5 (p -like) states subjected to uniaxial stress along the [001] or [111] crystallographic directions. At first, this problem appears to be a rather trivial extension of earlier stress studies¹⁴ of E_0 structure ($\Gamma_5 \rightarrow \Gamma_1$). In fact, the problem of rotating from

the x, y , and z cubic axes appropriate for [001] stress to a new set of axes with z along [111] is considerably more difficult in the present case. A general theoretical analysis of this problem by a method called "pseudorotation of angular momentum states" will be presented in a separate paper.¹⁵ Here we shall simply present the results which are used in Sec. IV for comparison with experiment and briefly discuss the more important features of the approach which point out the difference between the present case and the simple case mentioned above.

It is convenient to work with the T_d symmetry group for both the zinc-blende and diamond structures. In each case, T_d is the group of operations (site group) which does not involve the nonprimitive translation τ ($= \frac{1}{4}, \frac{1}{4}, \frac{1}{4}$). In the diamond structure, the factor group for Γ is O_h . It consists of T_d plus $T_d \times (J|\tau)$, where J is the inversion operator. The selection rules for O_h are trivially derived from T_d by treating the "parity" of a state under $(J|\tau)$ as an additional conserved quantum number.

The pseudorotation approach makes use of the close correspondence between the angular momentum functions $|j, m_j, s\rangle$, where s labels the parity (\pm) of the angular momentum state under J , and the irreducible representations of T_d . We introduce the notation $\psi_c^{jm_j s}$ to denote a function which transforms as the c irreducible representation of T_d and as the $|j, m_j, s\rangle$ angular momentum function of the full rotation group. For $j \leq \frac{3}{2}$, j is irreducible in T_d ; $j = 2, 3$ are reducible. This correspondence is most helpful when we attempt to rotate a function from the [001] to the [111] reference frame. Since this rotation is not an element of T_d , we rely upon the $|j, m_j, s\rangle$ character of a function to determine its rotational behavior.

Here we are concerned with $\Gamma_5 \rightarrow \Gamma_5$ transitions; i. e., transitions between p -like states. For comparison we also consider the $\Gamma_5 \rightarrow \Gamma_1$ transition from a p -like to an s -like state. When the spin-orbit interaction is included, we obtain the well-known result

$$\psi_1^{0+} \times \psi_6^{1/2+} = \psi_6^{1/2+} \quad (s\text{-like}), \quad (1)$$

$$\psi_5^{1-} \times \psi_6^{1/2+} = \psi_7^{1/2-} + \psi_8^{3/2-} \quad (p\text{-like}), \quad (2)$$

where the superscripts indicate the appropriate $|j, s\rangle$ values. Clearly the usual rules for parity and addition of angular momenta apply to the reduction of the product representations in Eqs. (1) and (2).

For cubic axes and a [001] stress, the results are straightforward. The tetragonal part of a [001] stress splits the $|\frac{3}{2}, \pm \frac{3}{2}\rangle$ and $|\frac{3}{2}, \pm \frac{1}{2}\rangle$ of ψ_6 as shown in Fig. 1. The optical selection rules shown in Fig. 1 can be obtained in a number of

ways: from the pseudorotation method,¹⁵ from Clebsch-Gordan coefficients,¹⁶ from the coupling coefficients of Koster *et al.*,¹⁰ or by direct computation using wave functions such as those given by Kane in Eq. (32) of Ref. 17. In the direct computation approach we use the fact that $\langle \psi_{5x} | P_y | \psi_{5z} \rangle$ is invariant for permutations of x, y , and z and zero for all other cases.

The optical transition strength is determined by matrix elements of the form

$$\langle \psi_a | \vec{A} \cdot \vec{P} | \psi_b \rangle = (\psi_a \psi_b^*, \vec{A} \cdot \vec{P}), \quad (3)$$

where $\psi_a \psi_b^*$, the outer product of the wave functions, is in general a reducible representation. As an example, consider the two cases of transitions from ψ_8 to ψ_6 or ψ_7 :

$$\psi_8^{3/2-} \psi_7^{1/2-} = \varphi_1^{0+} + \varphi_4^{1+} + \varphi_3^{2+} + \varphi_5^{2+}, \quad (4)$$

$$\psi_8^{3/2-} \psi_6^{1/2+} = \varphi_2^{0-} + \varphi_5^{1-} + \varphi_3^{2-} + \varphi_4^{2-}. \quad (5)$$

Since \vec{p} transforms as Γ_5^1 , only those terms which transform as φ_5 in Eqs. (4) and (5) contribute to the matrix element in Eq. (3). The important difference in the two cases is that φ_5^{2+} with $j=2$ rotational character contributes for $\psi_8 \leftrightarrow \psi_7$, whereas φ_5^{1-} with $j=1$ contributes for $\psi_8 \leftrightarrow \psi_6$. Thus the functions transform differently when they are "pseudorotated" to the [111] direction.

For the two examples given here it can be shown¹⁵ that the matrix element in Eq. (3) trans-

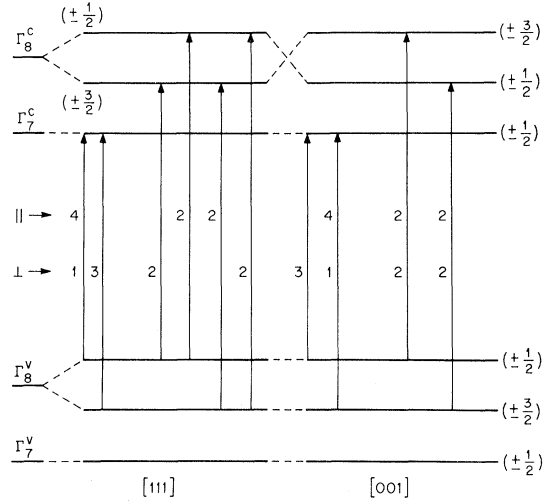


FIG. 1. Γ_5 conduction and valence bands are split by the spin-orbit interaction into Γ_8 ($j = \frac{3}{2}, m_j = \pm \frac{1}{2}, \pm \frac{3}{2}$) and Γ_7 ($j = \frac{1}{2}, m_j = \pm \frac{1}{2}$) states. A compressive uniaxial stress along [111] or [001] splits these states as shown for the deformation-potential constants d^v , b^v , d^c negative and b^c positive (hydrostatic effect not included). Allowed optical transitions are indicated by arrows. The relative transition strengths for polarization \parallel or \perp to the applied stress are given to the left of each arrow.

forms as

$$(\psi_{8R} \psi_{7R}^*, \vec{A} \cdot \vec{P}) = P_5^2 [G^2 \mathcal{R}^2 (\mathcal{R}^1)^{-1} A_R], \quad (6)$$

$$(\psi_{8R} \psi_{6R}^*, \vec{A} \cdot \vec{P}) = P_5^1 [G^1 A_R], \quad (7)$$

where ψ_R and A_R are the functions in the rotated frame, P_5^2 and P_5^1 are constants, \mathcal{R}^2 and \mathcal{R}^1 are rotation matrices for Γ_5 which depend upon the particular rotation being considered, and G^1 and G^2 are coupling matrices invariant with respect to rotations. The important result in Eq. (7) is that the functional form and resulting selection rules are the same for all reference frames. This is a direct consequence of the fact that the $j=1$ part of Eq. (5) contributes the transition strength. On the other hand, for $\psi_8 \leftrightarrow \psi_7$ or similarly for $\psi_8 \leftrightarrow \psi_6$ transitions the result [see Eq. (6)] depends upon the specific rotation. The results for these cases are given in Fig. 1 for both [001] and [111] stress. The numerical values to the left of the respective transition arrows are the relative transition strengths for \parallel and \perp polarization. The $\psi_8^{3/2 \pm 1/2}$ and $\psi_7^{1/2 \pm 1/2}$ states are mixed by the stress; however, for our purposes this mixing and the resulting nonlinearity of E vs stress are unimportant. Transitions from $\Gamma_7^v \rightarrow \Gamma_7^c$ are forbidden. Transitions from $\Gamma_7^v \rightarrow \Gamma_8^c$ (not shown in Fig. 1) have the same relative strengths and polarizations as those for $\Gamma_8^v \rightarrow \Gamma_7^c$.

The striking result in Fig. 1 is that the polarization behavior is significantly different for [001] and [111] stress directions. This contrasts with the result for the $\psi_8 \rightarrow \psi_6$ transition mentioned above, which is the same for the two stress directions. In fact it was this behavior observed for the 3.00-eV structure which prompted us to reconsider the theory of selection rules for Γ transitions.

For comparison with experiment we use the deformation-potential constants in Table I. We use Pollak and Cardona's experimental values¹⁴ for the valence band and Saravia and Brust's theoretical values¹⁸ for the conduction band. There is some scatter in the experimental values for b^v and d^v , but that is not important here. The important points are that there is reasonable agreement between experiment and theory for b^v and d^v ,

and that b^c is positive while the other three deformation-potential constants are negative. Figure 1 indicates the ordering of the states for compressive stress.

III. EXPERIMENTAL DETAILS

The data were obtained with a sensitive double-beam spectrophotometer described previously.¹⁹ For these experiments the peak-to-peak noise in the $(dR/dE)/R$ derivative data was 0.02 eV⁻¹ or less for a spectral resolution of approximately 1 meV. Uniaxial stress was applied with a pneumatic apparatus similar to one used for modulated piezoreflectance measurements. Here, dc stress was applied to a 1×1×10-mm sample submerged in pumped liquid helium. Copper end pads 5 mil thick were used at both ends of the samples to minimize the possible effects of any minor misalignment (no constraining end caps or Epoxy were used to mount the samples). Samples were cut from undoped single crystals of Ge with room-temperature resistivities of approximately 30 Ω cm. The samples were carefully lapped to obtain right parallelepipeds with the long axis along either a [111] or [001] crystallographic direction. The optical surface was Syton polished.²⁰

IV. RESULTS

Our reflectance data at 2 K for the E'_0 region are presented in Fig. 2(a). These data do not appear, at first, to be appreciably different from the 300 K results of Philipp and Taft.² However, if we consider the derivative data $(dR/dE)/R$ (obtained by a direct differentiation of the reflectance data with a digital computer) the difference between the 300- and 2-K data in Figs. 2(b) and 2(c) becomes quite apparent. At 2 K we observe two relatively sharp structures at 3.00 and 3.19 eV superimposed upon a rather broad background. At 150 K these features become quite broad; the peak-to-valley amplitude of the 3.19-eV structure is 0.04 eV⁻¹ and the 3.00-eV structure is barely visible above the noise. The background, on the other hand, is essentially the same at 2 and 300 K.

Stress data are presented in Fig. 3. We also illustrate, in the form of a bar graph, the behavior expected for $\Gamma_5^v \rightarrow \Gamma_5^c$ transitions on the basis of the symmetry results discussed in Sec. II. The lengths of the bars above (below) the horizontal base line represent the strengths of the respective transitions in \parallel (\perp) polarization. The energies of the lines, for the indicated levels of stress, are obtained by using the measured deformation-potential constants for Γ_5^v and the calculated values for Γ_5^c given in Table I. Hydrostatic shifts are not included in the bar graph. The observed stress behavior is in good agreement with the calculated behavior. This is our strongest evidence that the Γ assignment for these transitions

TABLE I. Deformation potentials for Γ_5 valence and conduction bands. Units are eV.

	Experiment ^a	Theory ^b
b^v	-2.6	-2.3
d^v	-4.7	-5.5
b^c		+1.2
d^c		-6.2

^aReference 14.

^bReference 18.

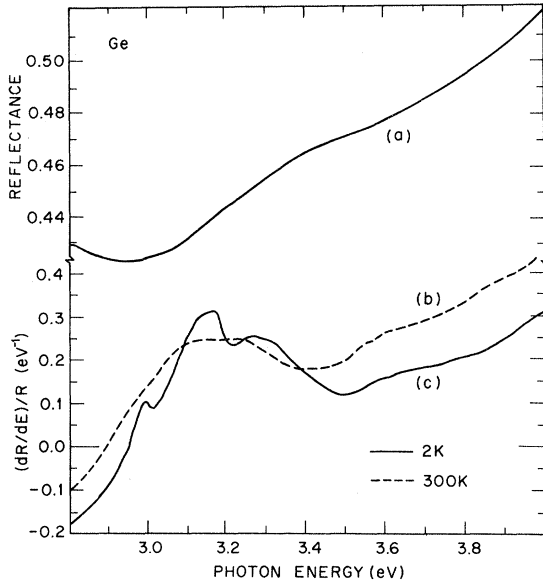


FIG. 2. (a) Reflectance spectrum of Ge at 2 K in the E_0' region; (b) and (c) logarithmic derivative data, $(dR/dE)/R$ at 300 and 2 K, respectively. The curve (c) is obtained from curve (a) by direct differentiation with a digital computer.

is correct.

One of the more striking results is that the polarizations for the 3.00-eV structure are reversed for [111] and [001] stress. The \parallel polarized line shifts downward for [111] and upward for [001] compressive stress, in agreement with the results in Fig. 1. For $\Gamma_8^v \rightarrow \Gamma_6^c$ (E_0 transitions) the line in \parallel polarization shifts to higher energy for both directions of compressive stress.¹⁴

Beyond this we obtain quantitative agreement for the magnitude of the splitting of the 3.00-eV structure. This result for [111] stress is demonstrated in Fig. 4. For a 5.2×10^9 -dyn-cm⁻² stress the observed splitting is 23 meV; the calculated value (for $d^v = -4.7$ eV) is 21 meV. Similarly for an [001] stress of 2.6×10^9 dyn cm⁻², the observed value is 13 meV; the calculated value (for $b^v = -2.6$ eV) is 17 meV.

The stress results for the 3.19-eV structure in Fig. 3, though less distinct than those for 3.00 eV, support the $\Gamma_8^v \rightarrow \Gamma_6^c$ assignment. For [111] stress the \parallel polarization is stronger than \perp . This agrees with the theoretical prediction that the energy shifts are large for the transitions seen in \perp polarization and small for those seen in \parallel polarization. The unresolved splitting for \perp polarization acts to broaden the structure and decrease its amplitude. For [001] stress small shifts are predicted for both polarizations. In this case, both the \perp and \parallel polarizations are essentially the same as the zero-stress result.

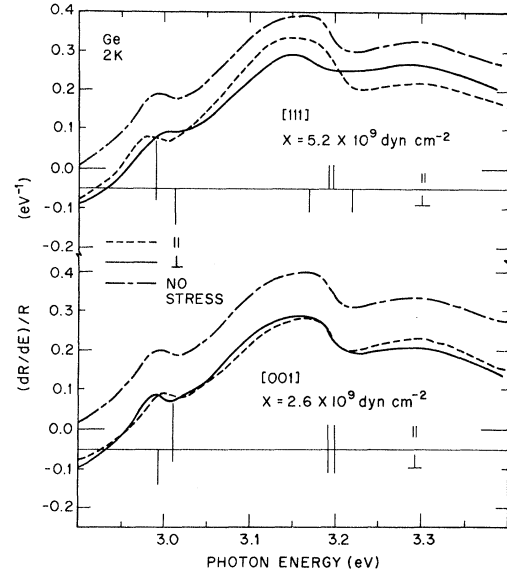


FIG. 3. Polarized data at 2 K for compressive axial stress. The dashed and solid curves are for light polarized parallel (\parallel) and perpendicular (\perp) to the stress axis, respectively. The data for no stress (dashed line) is displaced vertically by 0.1 eV^{-1} . The bar graphs represent the theoretical predictions based upon Fig. 1 and Table I for $\Gamma_8^v \rightarrow \Gamma_7^c$ and $\Gamma_8^v \rightarrow \Gamma_6^c$ transitions. See text for details.

This supports the idea that b^c is positive. If b^c were negative ($= -1.2 \text{ eV}$) the two transitions seen in \parallel and \perp polarization would be split by 24 meV. We would expect this splitting to decrease the derivative amplitude as it does in the case of \perp polarization for [111] stress.

To this point we have concentrated upon Γ symmetry and have shown that the data support a Γ assignment. Now let us consider whether the data are consistent with other symmetry assignments. In particular, are the data consistent with transitions from the twofold Δ_5 valence band to the Δ_1 conduction band which, according to band calcula-

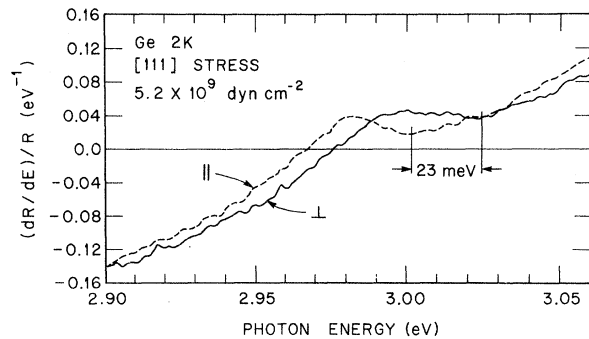


FIG. 4. Polarized data at 2 K for a compressive [111] stress of 5.2×10^9 dyn cm⁻².

tions,^{11,12} are to be found in this energy region? The behavior of the 3.00-eV structure for [111] stress is especially important in answering this question. In general a uniaxial stress can affect a transition away from Γ in two ways: It can split the degeneracy of a state in a given valley, or it can make the valleys inequivalent. The stress behavior for $\Delta_5 \leftrightarrow \Delta_1$ transitions is given by Kane in Tables III and IV of Ref. 21. For a [111] stress all six Δ regions remain equivalent. The observed splitting of the 3.00-eV structure rules out the possibility that the 3.00- and 3.19-eV structures arise from the spin-orbit splitting of the Δ_5 state. Furthermore, this assignment is unlikely on the grounds that the spin-orbit splitting along Δ should be small in germanium due to the forced degeneracy at the X point.²² Another possibility is that the spin-orbit splitting is negligible and that the 3.00-eV structure is the $\Delta_5 \rightarrow \Delta_1$ transition. In this case, for a [111] stress the qualitative behavior would be the same as that given in Fig. 1 for $\Gamma_8^v \rightarrow \Gamma_7^c$ transitions. However, for [001] stress, the transition should split into three levels; one seen in \parallel polarization and the other two seen in \perp polarization, each with $\frac{1}{2}$ the strength of the \parallel -polarized transition. It is more difficult to categorically rule out this possibility; however, there is strong evidence against it: (i) The [001] stress results in Fig. 3 do not indicate the more complicated three level splitting. (ii) The observed splittings agree with the values expected at Γ . (iii) This assignment does not account for the 3.19-eV structure which, on the basis of its strength, shape, and temperature dependence, appears to be closely related to the 3.00-eV structure.

Our data in Fig. 2(c) are quite similar to the 80-K transverse electroreflectance data of Fischer and co-workers¹³ except that their sharp structure at 3.00, 3.19, and 3.55 eV predominates over the broad background. This is to be expected since we are comparing our first-derivative results with the low-field electroreflectance which approximates a third derivative of the reflectance²³; thus, the sharper structure is enhanced more in the electroreflectance.

Fischer and co-workers assign the structure near 3.5 eV to the $\Gamma_7^v \rightarrow \Gamma_8^c$ transition ($\Gamma_7^v \rightarrow \Gamma_7^c$ is forbidden). This structure is too broad for us to obtain reliable stress results, but we do observe two features which suggest that this is not the $\Gamma_7^v \rightarrow \Gamma_8^c$ transition. First, the 3.5-eV structure is broad compared with that at 3.00 and 3.19 eV, but yet its derivative amplitude is comparable to, or greater than, the other two transitions. This indicates its transition strength is greater, which contradicts the theoretical result that the strengths for $\Gamma_8^v \rightarrow \Gamma_7^c$ and $\Gamma_7^v \rightarrow \Gamma_8^c$ transitions are the same. Second, the 3.5-eV structure does not shift or broaden appreciably at 300 K

(see Fig. 2). In contrast, the 3.00 and 3.19 eV transitions are broadened beyond observation at 300 K. Furthermore, the photoemission¹³ results indicate that $\Gamma_8^v \rightarrow \Gamma_7^c$ shifts 80 meV to lower energy as the temperature increases from 80 to 300 K. The 3.5-eV structure in Fig. 2 does not appear to shift with temperature.

V. DISCUSSION

Historically, the weak E'_0 structure in the early reflectance data was assigned⁸ as a Γ transition primarily because its energy agreed reasonably well with the $\Gamma_5^v \rightarrow \Gamma_5^c$ transition energy obtained from early band-structure calculations. More recently Cohen and co-workers^{11,12} have suggested, on the basis of band calculations and comparison with the wavelength-modulation data,⁶ that the E'_0 structure arises from transitions near the Δ -symmetry line. They argue that the small density of states at Γ makes this contribution unimportant. We believe these authors have overlooked two facts which tend to enhance the Γ structure, particularly at low temperatures. First, it is well known that Coulomb effects enhance M_0 critical point structure. Second, the structures which we identify as Γ transitions are enhanced because they are quite sharp; the widths are on the order of 20–30 meV at low temperatures.

It is quite possible that both Γ and Δ transitions contribute to the E'_0 region. We have concentrated upon the sharper structure, but we noted that this structure is superimposed upon a broader background structure. It is this background structure which was originally interpreted as Δ transitions. In fact, the sharper structures at 3.00 and 3.19 eV were not reported in the wavelength-modulation data of Zucca and Shen⁶ and of Braunstein and Welkowsky.⁷ Only the broader background structure near 3.2 eV was seen.

We would expect that Ge is not an isolated case in which this Γ structure is observable. It is possible, for example, that some of the structure seen in the 4.2–4.8-eV region of GaAs^{6,7,24} is due to Γ transitions. Braunstein and Welkowsky⁷ also mention this possibility for InSb. Furthermore, it is possible that studies of this region in other materials will observe additional sharp structure not previously seen.

ACKNOWLEDGMENTS

The authors gratefully acknowledge J. E. Rowe, S. E. Stokowski, and J. C. Hensel for helpful discussions, A. J. Williams for assistance with sample preparation, and H. C. Montgomery for the resistivity measurements.

¹This notation is discussed by M. Cardona, K. Shaklee, and F. H. Pollak [Phys. Rev. **154**, 696 (1967)] who also present in Fig. 1 the Ge reflectance data of H. Ehrenreich and H. R. Philipp, Phys. Rev. **129**, 1550 (1963).

²H. R. Philipp and E. A. Taft, Phys. Rev. **113**, 1002 (1959).

³M. Cardona and G. Harbeke, J. Appl. Phys. **34**, 813 (1963).

⁴R. F. Potter, Bull. Am. Phys. Soc. **12**, 320 (1967).

⁵A. K. Ghosh, Phys. Rev. **165**, 888 (1968).

⁶R. R. L. Zucca and Y. R. Shen, Phys. Rev. B **1**, 2668 (1970).

⁷R. Braunstein and M. Welkowsky, U. S. Atomic Energy Commission Technical Report No. CONF 700801, 1970, p. 439 (unpublished).

⁸H. Ehrenreich, H. R. Philipp, and J. C. Phillips, Phys. Rev. Letters **8**, 59 (1962); J. C. Phillips, Phys. Rev. **125**, 1931 (1962).

⁹M. Cardona and F. H. Pollak, Phys. Rev. **142**, 530 (1966).

¹⁰We use the T_d symmetry group for the Γ point ($k=0$) in germanium as discussed in Sec. II and adopt the notation of G. F. Koster, J. O. Dimmock, R. G. Wheeler, and H. Statz, *Properties of the Thirty-Two Point Groups* (MIT Press, Cambridge, Mass., 1963). Thus Γ_5^v , Γ_5^c , and Γ_1^c as used here correspond, respectively, to Γ_{15}^v , Γ_{15}^c , and Γ_1^c for T_d , and to $\Gamma_{25'}$, Γ_{15} , and Γ_2 for O_h in terms of the commonly used notation. Γ_5 is a threefold degenerate p -like state. Γ_1 is a nondegenerate s -like state.

¹¹J. P. Walter and M. L. Cohen, Phys. Rev. **183**, 763

(1969).

¹²R. N. Cahn and M. L. Cohen, Phys. Rev. B **1**, 2569 (1970).

¹³J. E. Fischer in Ref. 7, p. 427; T. M. Donovan, J. E. Fischer, J. Matsuzaki, and W. E. Spicer, Phys. Rev. B **3**, 4292 (1971).

¹⁴F. H. Pollak and M. Cardona, Phys. Rev. **172**, 816 (1968), and references to earlier work therein.

¹⁵E. O. Kane and D. D. Sell (unpublished).

¹⁶E. U. Condon and G. H. Shortley, *The Theory of Atomic Spectra* (Cambridge U. P., Cambridge, England, 1959), see Tables 1³-3³, p. 76.

¹⁷E. O. Kane, *Semiconductors and Semimetals*, edited by R. K. Willardson and A. C. Beer (Academic, New York, 1967), Vol. I, p. 75.

¹⁸L. R. Saravia and D. Brust, Phys. Rev. **178**, 1240 (1969). These authors give eigenvalues, but do not label the eigenstates. We identify the $m_j = \pm \frac{3}{2}$ states as those states with no second-order strain dependence and use the relations $\epsilon = (s_{11} - s_{12})X$ and $\epsilon = \frac{1}{2}s_{44}X$ for [001] and [111] stress, respectively. The deformation potentials are obtained from the energy splittings in Table III from the relations $\Delta E_{001} = 2b(s_{11} - s_{12})X$ and $\Delta E_{111} = ds_{44}X/\sqrt{3}$.

¹⁹D. D. Sell, Appl. Opt. **9**, 1926 (1970).

²⁰Syton is produced by the Monsanto Chemical Co.

²¹E. O. Kane, Phys. Rev. **178**, 1368 (1969).

²²L. R. Saravia and D. Brust, Phys. Rev. **176**, 915 (1968).

²³D. E. Aspnes and J. E. Rowe, in Ref. 7, p. 422.

²⁴D. D. Sell and S. E. Stokowski, in Ref. 7, p. 417.

First-Order Stark Effect in Phosphorus-Doped Silicon from Photoconductivity on Impurity Levels*

G. M. Guichar, C. Sebenne, F. Proix, and M. Balkanski

Laboratoire de Physique des Solides, Associé au Centre National de la Recherche Scientifique, Université Paris VI, Paris, France

(Received 14 July 1971)

Impurity-photoconductivity spectra at liquid-helium temperature on phosphorus-doped silicon reveal a shift of the threshold toward lower energies both as a function of the applied electric field and of the impurity concentration. The shift is proportional to the field and the proportionality coefficient goes through a maximum as the impurity concentration goes from 4×10^{16} to $1.2 \times 10^{18} \text{ cm}^{-3}$. The effect is interpreted as a first-order Stark effect due to a change in coupling between two phosphorus atoms which is largest when the phosphorus are neither tightly nor loosely coupled.

In a semiconductor at low-doping level, each impurity behaves as if it were alone in the host lattice: For example, substitutional phosphorus in silicon is characterized by a ground level at 45 meV below the conduction-band minimum and excited levels are well represented by the hydrogenic model. When the impurity concentration increases, an interaction occurs between neighbor impurities, at a doping level which depends on the semiconductor, and induces a decrease of the ionization energy. This effect has been observed in conductivity vs T

experiments, and for phosphorus in silicon good agreement between measurements and calculations has been obtained.^{1,2}

Now, when an electric field E is applied to the sample, the energy levels of an impurity atom are expected to change through the Stark effect. Kohn³ has shown that in a group-IV semiconductor doped with shallow impurities, when the hydrogenic model constitutes a good approximation, the Stark effect is of second order only. However, Kohn remarks that taking into account the full Hamiltonian of the